Supplementary Material for "Evidence for Singlet Fission Driven by Vibronic Coherence in Crystalline Tetracene"

Adrian F. Morrison and John M. Herbert*
Department of Chemistry, The Ohio State University, Columbus, OH 43210

I. PLANE-WAVE DFT CALCULATIONS

The unit cell for crystalline tetracene[1] was retrieved from the Cambridge Crystallographic Database and used as a starting point for geometry optimization via plane-wave DFT. As noted by Abdulla *et al.*,[2] lack of support for dispersion-corrected functionals for phonon calculations presents a major obstacle for studies of conjugated organic systems where these interactions play a key role. A crude yet serviceable workaround is to forgo the use of a generalized gradient approximation in favor of the local density approximation (LDA), as the latter has a tendency to overestimate binding energies, thus compensating for the absence of attractive dispersion interactions. All plane-wave DFT calculations were performed using the LDA functional and norm-conserving pseudopotentials.

Plane-wave DFT calculations were performed using the Quantum Espresso package.[3] Variable unit cell optimization was performed on the initial crystal structure under 1 atm of pressure with the SCF converged to a threshold of 10^{-9} a.u., mixing parameter $\beta = 0.7$, and kinetic energy cutoff of 60 Rydberg for the plane-wave basis. The Brillouin zone was sampled using a $2 \times 2 \times 1$ k-point mesh, and phonon modes were then computed for this optimized structure at the Γ point. The resulting phonon modes are in good agreement with previous work.[2] The asymmetric dimer in Fig. S1 constitutes the unit cell, and clearly shows the herringbone structure. Coordinates for this dimer are provided in Table S1 and phonon mode frequencies are listed in Table S2.

II. EXCITON MODEL CALCULATIONS

AIFDEM calculations were performed on the dimer in Fig. S1, using a locally-modified version of Q-Chem.[4] The exciton-site basis was constructed from monomer wave functions computed at the Hartree-Fock and configuration-interaction singles (CIS) levels, using the 6-31+G* basis set. In determinantal form, the triplet-pair basis states in Eq. (5) take the form

$$\begin{aligned}\big|^1\big(\Psi_A^{\rm T}\Psi_B^{\rm T}\big)\Psi_C\cdots\big\rangle = \sum_{i,a\in A}\sum_{j,b\in B} t^{ia}t^{jb}\bigg(&\frac{1}{\sqrt{3}}|\Phi_A^{\bar{i}a}\Phi_B^{j\bar{b}}\Phi_C\cdots\rangle + \frac{1}{\sqrt{3}}|\Phi_A^{i\bar{a}}\Phi_B^{\bar{j}b}\Phi_C\cdots\rangle - \frac{1}{\sqrt{6}}|\Phi_A^{ia}\Phi_B^{jb}\Phi_C\cdots\rangle \\ &+ \frac{1}{\sqrt{6}}|\Phi_A^{ia}\Phi_B^{\bar{j}\bar{b}}\Phi_C\cdots\rangle + \frac{1}{\sqrt{6}}|\Phi_A^{\bar{i}\bar{a}}\Phi_B^{jb}\Phi_C\cdots\rangle - \frac{1}{\sqrt{6}}|\Phi_A^{\bar{i}\bar{a}}\Phi_B^{\bar{j}\bar{b}}\Phi_C\cdots\rangle\bigg)\end{aligned} \tag{S1}$$

where overbars denote orbitals with β spin, and the singly-excited monomer amplitudes t^{ia} from Eq. (6) are spin-restricted. Matrix elements between non-orthgonal determinants such as $|\Phi_A^{\bar{i}a}\Phi_B^{j\bar{b}}\Phi_C\cdots\rangle$ are computed as in our previous work.[5]

AIFDEM calculations were performed using both a 25% and a 50% truncation threshold for the transformation between canonical molecular orbitals and natural transition orbitals (NTOs), or in other words insisting that we recover either 25% or 50% of the norm of the total transition vector, in the NTO basis. Eigenstates of the exciton Hamiltonian using either threshold are provided in Table S3 and are qualitatively similar when comparing the two thresholds. Non-adiabatic couplings $H_{JK}^{[x]}$, where J is the S_1 state, K is the multi-exciton state, and x is a nuclear Cartesian coordinate, are listed in Table S4 for a 25% NTO truncation threshold, and in Table S5 for a 50% truncation threshold. Projecting the plane-wave DFT phonon modes onto these couplings reveals which mode significantly modulate the derivative couplings, and this information is provided in Table S2 for both values of the NTO truncation threshold. Specifically, we list what percentage of the norm of the total nonadiabatic coupling vector is recovered by each phonon mode. This analysis clearly demonstrates that only a few modes are responsible for the overwhelming majority of the coupling.

* herbert@chemistry.ohio-state.edu

III. VIBRONIC MODEL HAMILTONIAN

For our vibronic simulations we utilize the well known Holstien-Peierls model.[6–11] The Hamiltonian is

$$\begin{aligned}\hat{\mathcal{H}} = &\sum_A |A\rangle \left[E_A + \sum_\alpha \omega_\alpha \left(\hat{a}_\alpha^\dagger \hat{a}_\alpha + \frac{1}{2} \right) + \frac{g_{AA\alpha}}{\sqrt{2}} \left(\hat{a}_\alpha^\dagger + \hat{a}_\alpha \right) \right] \langle A| \\ &+ \sum_A \sum_{B \neq A} |A\rangle \left(V_{AB} + \sum_\alpha \frac{g_{AB\alpha}}{\sqrt{2}} \left(\hat{a}_\alpha^\dagger + \hat{a}_\alpha \right) \right) \langle B|\end{aligned} \tag{S2}$$

in atomic units. Indices A and B refer to diabatic electronic states that in our model correspond to the exciton-site basis states of the AIFDEM. We include the states $|\Psi_A\Psi_B\rangle$, $|\Psi_A^*\Psi_B\rangle$, $|\Psi_A\Psi_B^*\rangle$, and $|^1(\mathrm{TT})\rangle$, and the electronic AIFDEM Hamiltonian is initially subjected to symmetric (Löwdin) orthogonalization. The operators $\hat{a}_\alpha$ and $\hat{a}_\alpha^\dagger$ are harmonic oscillator raising and lowering operators for phonon mode α, whose frequency is ω_α. Our simulations, however, are limited to a single mode with $\omega = 1432.19$ cm^{-1}, as computed via plane-wave DFT, and only the $|0\rangle$ and $|1\rangle$ states of the oscillator are included in the basis.

Diagonal entries E_A represent the exciton-site energies. The AIFDEM lacks intramolecular dynamical electron correlation and therefore does not reproduce the known singlet/triplet gap in tetracene, so for the purpose of the Redfield dynamics simulations the computed site energies were corrected to match experimental values of the $S_0 \rightarrow S_1$ excitation energy and the S_0/T_1 gap. (Similar corrections have been used in RAS-2SF calculations,[12,13] for the same reason: these calculations are capable of describing the coupled triplet pair but also lack dynamical electron correlation. This amounts to shifting E_A downwards by 12,251.6 cm^{-1} for single-exciton eigenstates and downward by 11,533.7 cm^{-1} for the multi-exciton eigenstate. The electronic coupling elements V_{AB} in Eq. (S2) were taken directly from the orthogonalized AIFDEM Hamiltonian.

The quantities $g_{AA\alpha}$ and $g_{AB\alpha}$ are electron-phonon coupling constants of the local (Holstein) and non-local (Peierls) type, respectively. To compute these couplings we first symmetrically orthogonalize the AIFDEM derivatives couplings, including the derivative of the orthogonalization transformation. (Details of how to take the derivative of Löwdin's symmetric orthogonalization transformation can be found in Ref. 14.) The orthogonalized derivatives are then transformed from atomic Cartesian coordinates, in which they are initially computed, to the dimensionless spectroscopic coordinates corresponding to normal modes:

$$g_{AB\alpha} = \frac{1}{\sqrt{\mu_\alpha \omega_\alpha}} \sum_x H_{AB}^{[x]} D_{x\alpha} \ . \tag{S3}$$

Here, the αth column of the matrix $\mathbf{D}$ contains the normalized Cartesian displacements corresponding to normal mode α, and μ_α is its effective mass. Following this transformation, the electron/phonon couplings, which are in practice matrix elements of the vibronic Hamiltonian, have appropriate dimensions of energy.

Redfield dynamics simulations for the model Hamiltonian in the indicated basis were performed using the QuTip program.[15]

[1] D. Holmes, S. Kumaraswamy, A. J. Matzger, and K. P. C. Vollhardt, CCDC 114446: Experimental Crystal Structure Determination (1999), Deposited on: 8/2/1999.
[2] M. Abdulla, K. Refson, R. H. Friend, and P. D. Haynes, J. Phys.: Condens. Matt. **27**, 375402:1 (2015).
[3] P. Giannozzi et al., J. Phys: Condens. Matt. **21**, 395502:1 (2009).
[4] Y. Shao et al., Mol. Phys. **113**, 184 (2015).
[5] A. F. Morrison, Z.-Q. You, and J. M. Herbert, J. Chem. Theory Comput. **10**, 5366 (2014).
[6] K. Hannewald and P. A. Bobbert, Appl. Phys. Lett. **85**, 1535 (2004).
[7] A. Troisi and G. Orlandi, Phys. Rev. Lett. **96**, 086601:1 (2006).
[8] A. Troisi, Adv. Mater. **19**, 2000 (2007).
[9] V. Coropceanu et al., Chem. Rev. **107**, 926 (2007).
[10] A. Girlando et al., Phys. Rev. B **82**, 035208:1 (2010).
[11] A. Zhugayevych and S. Tretiak, Annu. Rev. Phys. Chem. **66**, 305 (2015).
[12] P. M. Zimmerman, C. B. Musgrave, and M. Head-Gordon, Acc. Chem. Res. **46**, 1339 (2013).
[13] X. Feng, A. V. Luzanov, and A. I. Krylov, J. Phys. Chem. Lett. **4**, 3845 (2013).
[14] A. F. Morrison and J. M. Herbert, Analytic derivative couplings and electron/phonon couplings for an *ab initio* Frenkel-Davydov exciton model, with application to triplet exciton mobility in crystalline tetracene, (in preparation), 2017.
[15] J. R. Johansson, P. D. Nation, and F. Nori, Comput. Phys. Commun. **184**, 1234 (2013).

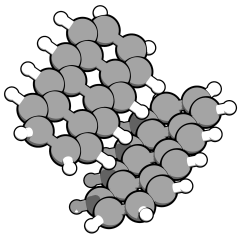

FIG. S1: Tetracene dimer extracted from the optimized crystal structure and used for subsequent AIFDEM calculations.

TABLE S1: Optimized geometry of the crystalline tetracene unit cell (dimer).

atom	x	y	z	atom	x	y	z
C	1.10179	4.81008	−4.73772	C	−2.32282	1.63662	−4.50776
C	0.15871	4.26741	−3.92745	C	−3.21899	1.65149	−3.49145
C	0.37922	4.14461	−2.53904	C	−2.93377	1.00115	−2.27384
C	−0.55307	3.57764	−1.69601	C	−3.83808	0.97847	−1.23419
C	−0.32233	3.46244	−0.32808	C	−3.56010	0.31552	−0.04378
C	−1.25933	2.89562	0.53050	C	−4.47188	0.27949	1.00699
C	−1.02206	2.78519	1.88432	C	−4.18288	−0.36890	2.18822
C	−1.96559	2.20709	2.75809	C	−5.08664	−0.38053	3.27138
C	−1.71759	2.11526	4.08758	C	−4.76639	−1.00289	4.43120
C	−0.50647	2.59193	4.62443	C	−3.53195	−1.66582	4.56887
C	0.43661	3.13460	3.81416	C	−2.63577	−1.68069	3.55255
C	0.21610	3.25740	2.42575	C	−2.92100	−1.03035	2.33495
C	1.14839	3.82437	1.58271	C	−2.01669	−1.00768	1.29529
C	0.91765	3.93957	0.21479	C	−2.29467	−0.34473	0.10488
C	1.85465	4.50639	−0.64380	C	−1.38288	−0.30870	−0.94588
C	1.61738	4.61682	−1.99761	C	−1.67189	0.33969	−2.12711
C	2.56091	5.19492	−2.87139	C	−0.76813	0.35133	−3.21028
C	2.31290	5.28675	−4.20088	C	−1.08837	0.97368	−4.37010
H	0.91521	4.88574	−5.81056	H	−2.56426	2.13780	−5.44540
H	−0.79274	3.91225	−4.32767	H	−4.17920	2.15937	−3.60059
H	−1.49473	3.20942	−2.10806	H	−4.79819	1.48656	−1.34815
H	−2.20424	2.53117	0.12120	H	−5.43284	0.78721	0.89474
H	−2.90117	1.83838	2.33679	H	−6.04433	0.13001	3.15570
H	−2.46090	1.66217	4.74486	H	−5.46728	−0.98841	5.26790
H	−0.31989	2.51626	5.69727	H	−3.29051	−2.16700	5.50650
H	1.38805	3.48975	4.21437	H	−1.67557	−2.18857	3.66169
H	2.09005	4.19259	1.99477	H	−1.05658	−1.51576	1.40925
H	2.79955	4.87083	−0.23449	H	−0.42193	−0.81641	−0.83364
H	3.49649	5.56363	−2.45008	H	0.18956	−0.15922	−3.09460
H	3.05622	5.73984	−4.85815	H	−0.38749	0.95921	−5.20680

TABLE S2: Normal mode frequencies (in cm^{-1}) and percentage of the nonadiabatic coupling projection.

Mode	Freq.	% of coupling		Mode	Freq.	% of coupling		Mode	Freq.	% of coupling	
		25% NTO[a]	50% NTO[b]			25% NTO[a]	50% NTO[b]			25% NTO[a]	50% NTO[b]
1	53.67	0.04	0.03	59	770.25	0.00	0.00	117	1306.73	0.35	0.71
2	69.86	0.18	0.19	60	774.71	0.05	0.03	118	1307.81	0.05	0.01
3	80.96	0.00	0.00	61	780.99	0.00	0.02	119	1326.01	0.24	0.28
4	101.51	0.00	0.00	62	782.65	0.01	0.01	120	1331.41	0.00	0.00
5	103.99	0.11	0.04	63	782.82	0.01	0.01	121	1376.44	0.00	0.00
6	119.02	0.01	0.00	64	788.38	0.00	0.00	122	1381.08	0.02	0.01
7	136.31	0.03	0.00	65	835.06	0.00	0.00	123	1399.32	1.74	0.04
8	147.96	0.01	0.00	66	839.11	0.01	0.00	124	1404.17	0.32	0.00
9	152.79	0.02	0.01	67	840.38	0.00	0.00	125	1412.63	0.01	0.00
10	161.08	0.00	0.01	68	852.78	0.23	0.24	126	1413.25	0.47	0.76
11	169.92	0.01	0.00	69	854.71	0.01	0.00	127	1432.19	26.90	27.26
12	172.20	0.00	0.00	70	855.49	2.11	1.97	128	1434.08	11.55	14.12
13	180.74	0.01	0.02	71	868.41	0.38	0.42	129	1439.99	0.37	0.09
14	182.36	0.01	0.01	72	871.27	0.01	0.00	130	1440.63	0.14	0.00
15	223.31	0.00	0.00	73	891.62	0.00	0.00	131	1451.91	0.07	0.02
16	228.64	0.00	0.00	74	891.90	0.00	0.00	132	1454.72	0.50	0.36
17	274.45	0.00	0.00	75	895.25	0.00	0.01	133	1459.51	0.62	0.47
18	282.42	0.00	0.00	76	896.24	0.02	0.07	134	1463.87	0.03	0.02
19	303.44	0.22	0.08	77	910.60	0.02	0.00	135	1475.26	0.37	0.24
20	304.28	0.01	0.00	78	913.30	0.01	0.00	136	1477.13	0.00	0.00
21	318.67	0.02	0.05	79	921.93	0.00	0.00	137	1536.86	19.36	19.05
22	325.17	0.00	0.01	80	926.82	0.00	0.00	138	1539.89	13.17	18.13
23	329.97	0.00	0.00	81	928.55	0.00	0.00	139	1559.22	1.50	0.53
24	332.51	0.01	0.00	82	929.30	0.24	0.11	140	1564.22	0.00	0.33
25	392.72	0.00	0.00	83	959.49	0.00	0.00	141	1564.94	0.11	0.58
26	397.54	0.00	0.00	84	962.49	0.00	0.00	142	1567.89	0.16	0.01
27	436.65	0.12	0.05	85	962.91	0.01	0.00	143	1580.55	0.20	0.26
28	438.20	0.09	0.03	86	964.97	0.00	0.01	144	1583.70	0.00	0.00
29	460.44	0.01	0.00	87	975.04	0.01	0.00	145	1628.80	0.00	0.00
30	471.72	0.00	0.00	88	981.78	0.00	0.00	146	1633.73	0.20	0.01
31	479.01	0.00	0.00	89	983.88	0.01	0.00	147	1634.41	3.17	0.15
32	483.96	0.02	0.00	90	988.49	0.00	0.00	148	1638.34	0.03	0.00
33	487.53	0.00	0.00	91	1013.49	0.11	0.07	149	1651.22	0.58	0.67
34	493.45	0.02	0.00	92	1014.92	0.99	0.97	150	1654.52	0.00	0.02
35	497.16	0.03	0.10	93	1016.20	0.00	0.00	151	3045.06	0.00	0.00
36	499.11	0.00	0.00	94	1016.73	0.62	0.70	152	3048.49	0.00	0.00
37	508.13	0.00	0.00	95	1116.40	0.01	0.01	153	3048.91	0.00	0.00
38	515.38	0.00	0.00	96	1117.82	0.04	0.05	154	3049.05	0.00	0.00
39	554.09	0.05	0.02	97	1121.46	0.02	0.00	155	3049.36	0.00	0.00
40	557.80	0.02	0.01	98	1123.62	0.00	0.00	156	3049.65	0.00	0.00
41	568.27	0.00	0.00	99	1127.33	0.11	0.00	157	3051.26	0.00	0.00
42	573.03	0.00	0.00	100	1136.49	0.02	0.00	158	3052.40	0.00	0.00
43	611.93	0.01	0.09	101	1137.04	0.22	0.14	159	3053.13	0.04	0.05
44	614.57	0.01	0.05	102	1146.23	0.11	0.17	160	3054.34	0.07	0.11
45	621.34	0.07	0.10	103	1152.19	0.44	0.01	161	3056.79	0.00	0.00
46	622.36	0.03	0.02	104	1153.55	0.06	0.01	162	3057.27	0.02	0.01
47	628.21	0.02	0.03	105	1163.50	0.23	0.01	163	3057.65	0.05	0.06
48	628.29	0.05	0.04	106	1165.26	0.01	0.01	164	3057.90	0.01	0.00
49	730.59	0.00	0.00	107	1198.39	0.27	0.28	165	3059.50	0.00	0.01
50	731.17	0.00	0.00	108	1200.36	0.04	0.04	166	3060.04	0.01	0.01
51	732.66	0.00	0.00	109	1201.83	7.03	6.78	167	3062.67	0.00	0.00
52	735.60	0.00	0.00	110	1202.83	0.24	0.55	168	3063.27	0.07	0.10
53	739.80	0.01	0.00	111	1255.88	0.13	0.10	169	3064.60	0.03	0.04
54	750.26	0.02	0.00	112	1257.09	0.00	0.00	170	3064.67	0.00	0.00
55	759.94	0.34	0.30	113	1257.94	0.00	0.00	171	3074.15	0.09	0.12
56	760.86	0.05	0.01	114	1258.62	0.03	0.02	172	3075.62	0.04	0.01
57	762.27	0.24	0.03	115	1299.38	0.10	0.14	173	3075.74	0.19	0.17
58	762.56	0.47	0.10	116	1303.03	0.01	0.00	174	3075.99	0.04	0.06

[a]Retaining 25% of the total norm of the NTOs

[a]Retaining 50% of the total norm of the NTOs

TABLE S3: Eigenvectors for tetracene dimer in the non-orthogonal exciton-site basis.

25 % NTO Threshold

Eigenstate	$\|\Xi_{S_0}\rangle$	$\|\Xi_{S_1}\rangle$	$\|\Xi_{S_2}\rangle$	$\|\Xi_{TT}\rangle$
Excitation Energy (eV)		2.30	2.37	2.53
Oscillator Strength		0.1932	0.3776	0.0
Basis State	Eigenvector Coefficient			
$\|\Psi_A\Psi_B\rangle$	0.9967	−0.0642	0.0502	−0.0010
$\|\Psi_A^*\Psi_B\rangle$	−0.0502	−1.0173	−0.2605	−0.0031
$\|\Psi_A\Psi_B^*\rangle$	0.0686	0.2574	−1.0174	0.0054
$\|^1(\mathrm{TT})\rangle$	−0.0005	0.0050	−0.0052	−1.2193

50 % NTO Threshold

Eigenstate	$\|\Xi_{S_0}\rangle$	$\|\Xi_{S_1}\rangle$	$\|\Xi_{S_2}\rangle$	$\|\Xi_{TT}\rangle$
Excitation Energy (eV)		2.30	2.36	2.50
Oscillator Strength		0.1142	0.2078	0.0
Basis State	Eigenvector Coefficient			
$\|\Psi_A\Psi_B\rangle$	0.9982	0.0476	0.0353	0.0020
$\|\Psi_A^*\Psi_B\rangle$	0.0375	−0.9942	0.2271	−0.0087
$\|\Psi_A\Psi_B^*\rangle$	0.0466	−0.2254	−0.9942	−0.0111
$\|^1(\mathrm{TT})\rangle$	−0.0010	−0.0118	−0.0097	1.1139

TABLE S4: Nonadiabatic coupling vector (in a.u.) using a 25% NTO truncation threshold.

atom	x	y	z	atom	x	y	z
C	0.02100	−0.02757	0.16775	C	0.10358	−0.12173	0.16509
C	0.19179	0.02927	0.25526	C	0.21218	−0.18228	0.21657
C	0.63195	0.43264	−0.58823	C	0.70768	−0.00708	−0.80211
C	−0.30519	−0.28779	0.63657	C	−0.31353	−0.17184	0.76639
C	−0.65980	−0.19976	−0.33843	C	−0.69541	0.32954	−0.05098
C	0.10671	0.07588	−0.81563	C	0.12703	0.33594	−0.90593
C	0.07336	−0.19846	0.95791	C	0.19196	−0.55775	1.06989
C	0.29797	0.13192	−0.09437	C	0.35392	−0.00980	−0.34702
C	0.04476	0.04864	−0.02294	C	0.28100	−0.16420	0.00457
C	0.02224	0.04370	−0.24636	C	−0.31568	0.16945	−0.01639
C	−0.20167	−0.07872	−0.11337	C	−0.07993	0.27753	−0.39313
C	−0.43380	−0.28906	0.40450	C	−0.74163	−0.05135	0.88778
C	0.28024	0.14057	−0.35481	C	0.35884	0.20459	−0.77654
C	0.76584	0.41155	−0.01680	C	0.69785	−0.32606	0.02170
C	−0.22952	−0.27373	0.98433	C	−0.12755	−0.27780	0.94861
C	−0.41658	0.21476	−2.59315	C	−0.20841	0.55950	−1.02480
C	−0.75712	−0.31287	0.37801	C	−0.33608	0.07240	0.25286
C	−0.53065	−0.33027	0.11229	C	−0.16893	0.05827	0.05588
H	−0.00419	0.01253	−0.00350	H	−0.00112	−0.00055	−0.00299
H	−0.01074	0.01374	−0.00637	H	−0.00535	0.00321	−0.00188
H	−0.00188	0.01332	0.01203	H	0.00756	−0.00619	0.00852
H	0.00298	0.02763	0.00027	H	0.01159	−0.00289	−0.00879
H	−0.01020	0.00554	−0.00067	H	−0.00655	0.00294	−0.00004
H	−0.00087	−0.00167	0.00080	H	0.00003	−0.00368	0.00242
H	0.00105	0.00030	0.00224	H	−0.00076	0.00091	0.00166
H	0.00289	0.00326	0.00126	H	0.00173	−0.01043	−0.00082
H	−0.01098	−0.00072	−0.00952	H	−0.00729	0.00652	−0.01022
H	−0.01066	−0.01148	0.00676	H	−0.01268	0.00138	0.00704
H	0.00595	0.00183	0.00002	H	0.00457	−0.00490	−0.00071
H	−0.00056	0.00427	−0.00009	H	−0.00086	−0.00265	−0.00374

TABLE S5: Nonadiabatic coupling vector (in a.u.) using a 50% NTO truncation threshold.

atom	x	y	z	atom	x	y	z
C	−0.05021	−0.04935	0.33738	C	0.38397	−0.28726	0.22479
C	0.39801	0.07917	0.44352	C	0.38960	−0.48138	0.68293
C	1.05287	0.62966	−1.19994	C	1.65765	0.04404	−1.96014
C	−0.69303	−0.48531	1.21856	C	−0.79431	−0.38381	1.77480
C	−1.54914	−0.67702	−0.47284	C	−1.50209	0.73688	−0.04662
C	0.28439	0.46513	−1.48900	C	0.27696	0.75338	−2.05299
C	0.25500	−0.10719	1.73058	C	0.57992	−1.26406	2.33771
C	0.55708	0.25833	0.14393	C	0.74531	−0.11258	−0.56860
C	0.12765	0.09940	−0.53122	C	0.45491	−0.16054	−0.13805
C	0.19279	0.11848	−0.32741	C	−0.29004	0.26746	−0.28325
C	−0.48896	−0.12220	−0.44789	C	−0.47029	0.44558	−0.65419
C	−1.27871	−0.78895	1.32314	C	−1.76092	−0.06212	2.01749
C	0.68319	0.61150	−1.60061	C	0.80328	0.40872	−1.90918
C	1.38079	0.41090	1.01228	C	1.44112	−0.78644	0.23178
C	−0.09172	−0.23086	1.22630	C	−0.21110	−0.73296	1.89340
C	−0.56903	0.44765	−4.36804	C	−0.50720	1.23894	−2.26993
C	−0.98815	−0.52283	−0.07502	C	−0.73674	0.09488	0.54980
C	−0.91672	−0.42402	0.44792	C	−0.46780	0.18458	0.09895
H	−0.00404	−0.00220	−0.01628	H	0.00195	0.00284	−0.00595
H	−0.00672	−0.00870	−0.00631	H	−0.01340	0.00697	−0.00344
H	0.01320	0.01089	0.02804	H	0.01681	−0.01434	0.02143
H	0.01950	0.02166	−0.00622	H	0.02416	−0.00671	−0.01913
H	−0.01282	0.00045	0.00405	H	−0.01446	0.00776	0.00120
H	−0.00829	−0.00305	−0.00040	H	−0.00425	−0.00449	0.00439
H	0.00557	0.00375	0.00518	H	−0.00211	−0.00262	0.00739
H	0.00769	0.00663	0.01416	H	0.01866	−0.00038	0.00899
H	−0.00894	−0.00133	−0.02564	H	−0.01301	0.01626	−0.01989
H	−0.02486	−0.00636	0.00495	H	−0.02313	0.00751	0.01769
H	0.01148	0.00618	0.00012	H	0.01507	−0.00829	−0.00145
H	0.00831	−0.00174	−0.00114	H	0.00260	0.00239	−0.00511